

# Lithium–Sulfur Cell Equivalent Circuit Network Model Parameterization and Sensitivity Analysis

Abbas Fotouhi, *Member, IEEE*, Daniel J. Auger, *Senior Member, IEEE*, Karsten Propp, Stefano Longo, *Senior Member, IEEE*, Rajlakshmi Purkayastha, Laura O’Neill, and Sylwia Walus

**Abstract**—Compared to lithium-ion batteries, lithium–sulfur (Li-S) batteries potentially offer greater specific energy density, a wider temperature range of operation, and safety benefits, making them a promising technology for energy storage systems especially in automotive and aerospace applications. Unlike lithium-ion batteries, there is not a mature discipline of equivalent circuit network (ECN) modelling for Li-S. In this study, ECN modelling is addressed using formal ‘system identification’ techniques. A Li-S cell’s performance is studied in the presence of different charge/discharge rates and temperature levels using precise experimental test equipment. Various ECN model structures are explored, considering the tradeoffs between accuracy and speed. It was concluded that a ‘2RC’ model is generally a good compromise, giving good accuracy and speed. Model parameterization is repeated at various state-of-charge (SOC) and temperature levels, and the effects of these variables on Li-S cell’s ohmic resistance and total capacity are demonstrated. The results demonstrate that Li-S cell’s ohmic resistance has a highly nonlinear relationship with SOC with a break-point around 75% SOC that distinguishes it from other types of battery. Finally, an ECN model is proposed which uses SOC and temperature as inputs. A sensitivity analysis is performed to investigate the effect of SOC estimation error on the model’s accuracy. In this analysis, the battery model’s accuracy is evaluated at various SOC and temperature levels. The results demonstrate that the Li-S cell model has the most sensitivity to SOC estimation error around the break-point (around 75% SOC) whereas in the middle SOC range, from 20% to 70%, it has the least sensitivity.

**Index Terms**—Battery modelling, identification, lithium-sulfur cell, state-of-charge estimation, sensitivity analysis.

## NOMENCLATURE

$C_1$	Battery polarization capacitance.
$C_t$	Battery total capacity.
$i(t)$	Battery current.

Manuscript received June 11, 2016; revised January 20, 2017; accepted February 22, 2017. Date of publication April 18, 2017; date of current version September 15, 2017. This work was funded as part of the “Revolutionary Electric Vehicle Battery” (REVB) project, co-funded by Innovate UK and EPSRC (TS/L000903/1 and EP/L505286/1), and the “Understanding Future Vehicles” project funded by EPSRC (EP/I038586/1). (*Corresponding author: Abbas Fotouhi.*)

A. Fotouhi, D. J. Auger, K. Propp, and S. Longo are with the Advanced Vehicle Engineering Centre, Cranfield University, Bedfordshire MK43 0AL, U.K. (e-mail: a.fotouhi@cranfield.ac.uk; abfotouhi@gmail.com; d.j.auger@cranfield.ac.uk; k.propp@cranfield.ac.uk; s.longo@cranfield.ac.uk).

R. Purkayastha, L. O’Neill, and S. Walus are with OXIS Energy, Culham Science Centre, Oxfordshire OX14 3DB, U.K. (e-mail: Raj@oxisenergy.com; Laura.O’Neill@oxisenergy.com; Sylwia.Walus@oxisenergy.com).

Color versions of one or more of the figures in this paper are available online at <http://ieeexplore.ieee.org>.

Digital Object Identifier 10.1109/TVT.2017.2678278

$I_L$	Battery load current.
$L_2$	Root mean square error (RMSE).
$L^\infty$	Maximum error value.
$P_i$	A parameter of the battery model.
$R_{\text{int}}$	Battery internal (total) resistance.
$R_1$	Battery polarization resistance.
$R_O$	Battery ohmic resistance.
SOC	Battery state-of-charge.
T	Temperature.
$V_{OC}$	Battery open circuit voltage.
$V_t$	Battery terminal voltage.
$y(t_k)$	Real output at time $k$ .
$\hat{y}(t_k t_{k-1}; \theta)$	Predicted value of the output at time $k$ using the parameter vector $\theta$ .
$\varepsilon$	Prediction error.
$\gamma$	Battery coulombic efficiency.
$\theta$	Model’s parameter vector.

## I. INTRODUCTION

THE development of electrical energy storage systems plays a key role in the vehicle electrification process. Lithium-ion (Li-ion) batteries are the most common and well-known technologies used in present-day electric vehicles (EVs). Achieving specific energy densities up to 200–250 W·h/kg [1], Li-ion batteries provide a typical electric vehicle to achieve a range of 250 km with a reasonable and efficient battery size [2]. This does not compare well with the range of a gasoline or diesel powered vehicle, so there is a strong incentive to explore new technologies with the potential to achieve much higher energy densities. Lithium-sulfur (Li-S) batteries have realistic near-future prospects of achieving energy densities up to 650 W·h/kg [3], and as a result, they are one of the many technologies under consideration for next generation EVs. In addition, when compared to Li-ion, Li-S battery has other advantages such as good low-temperature performance, and inexpensive and nontoxic raw materials [4]. Li-S also operates over a wider temperature range and it is safer than Li-ion. These properties are seen as well suited to automotive application. Conversely, present-day Li-S battery technology suffers from significant limitations such as low power capability, low cycle life and a volumetric energy density that is no better than Li-ion. It is too early to know whether materials science will resolve some of these problems, but at present, they are ongoing research efforts exploring the chemistry.

Regardless of the state of development of the chemistry, it is important to be able to operate Li-S cells in practical applications, and this study is focused on building a fast low-fidelity model for a Li-S cell. In an EV, it is important to understand state-of-charge (SOC) (or remaining capacity), which is vital for any kind of range prediction. An optimal use of a battery depends on efficient and accurate battery modelling. Different approaches can be used for cell modelling: the two main groupings are (i) electrochemical models, and (ii) equivalent (electrical) circuit network (ECN) models. Electrochemical battery models are high-fidelity models working based on solving complex mathematical equations (e.g. partial differential equations) and attempting to fully describe the electrochemical reactions taking place inside a cell. On the other hand, ECN models only focus on reproducing the transient terminal voltage of the battery with basic electronic components like resistors or capacitors. Therefore they are mathematically simpler, faster and more suitable for real-time applications, though they provide less physical insight. There are also other modelling approaches in the literature which are reviewed in [5]. Because of the low computational effort and relatively good precision, ECN models have been the subject of studies in a wide range specifically for automotive application [6]–[8]. Unlike Li-ion batteries—where ECN models are commonly discussed—there are few studies in the literature proposing or using equivalent circuit models for Li-S batteries.

In [9] and [10], impedance spectroscopy has been used to investigate Li-S cell's properties. Then parameters of a second-order electrical circuit model were determined based on the spectrum data. Although the authors have touched briefly on the subject of ECN modelling of a Li-S cell; their study was more focused on Li-S cell cycling analysis. The model parameterization method that was used in [9] and [10], i.e. impedance spectroscopy, is different from the system identification approach which is used in this study. The advantage of the system identification technique, which is proposed here, is its higher speed that enables us to use it in online applications such as EV battery management system (BMS). In another study, done by Knapp *et al.* [11], Li-S cell's performance was investigated using an ECN model by considering various model structures subjected to discharge pulses in the whole range of SOC. The battery model's parameters, i.e. ohmic resistance and capacitance, were obtained vs. SOC and discharge rates [11]. However, the effects of temperature and charging pulses were not considered in [11], which are covered in this study.

In this study, ECN modelling of a Li-S cell is performed with a focus on real-time fast model parameterization using a system identification technique. Li-S cell's charge/discharge behaviour is investigated subject to various C-rates using precise experimental test equipment. The effect of temperature is also assessed by repeating the tests at 10, 20, 30, 40 and 50 °C. So, the first contribution of this study is development of an ECN charge/discharge model for a Li-S cell by considering SOC and temperature effects. Model parameterization is performed at various charge and temperature levels demonstrating the effects of these variables on cell's ohmic resistance and capacitance. The second contribution of this study is an appropriate compromise between accuracy and simplicity (speed) of the model.

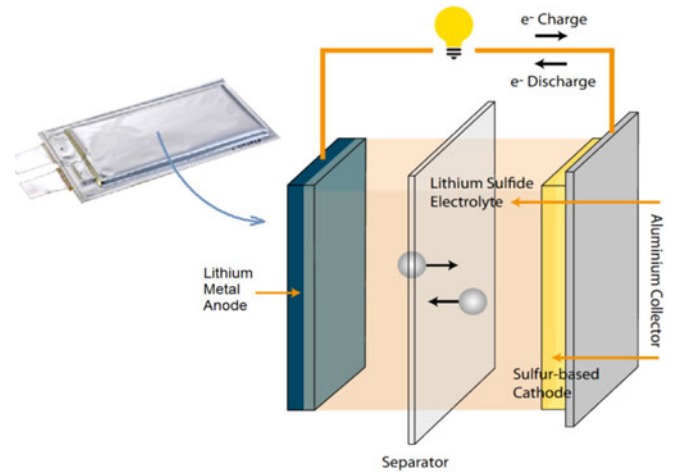


Fig. 1. OXIS Li-S cell (left) and schematic of inside the cell (right) [12].

TABLE I  
SPECIFICATIONS OF OXIS LITHIUM-SULFUR CELL

Type	Rechargeable lithium-sulfur pouch cell Li Metal Anode
Nominal dimension	145 mm × 78 mm × 5.6 mm
Applications	Recommended discharge current: 680 mA
Nominal voltage	2.05 V
Capacity	Typical: 3400 mA·h when discharged at 680 mA at 1.5 V at 30 °C
Charging condition	340 mA to 2.45 V at 30 °C
Recommended charging condition in applications	340 mA constant current (C/10) Charge termination control recommended: CC stop at 2.45 V or 11 h max charge time
Clamped charging voltage	2.45 ± 0.05 V
Service life	> 95 cycles at 100% depth of discharge > 150 cycles at 80% depth of discharge
Weight	Approx. 50.7 g
Ambient temperature range	Charge/ Discharge: 5 to 80 °C Storage (1 year): -27 to 30 °C

Four ECN model structures with different levels of complexity are evaluated for this purpose. The third contribution of this study is a sensitivity analysis which is performed to investigate the effect of SOC estimation error on ECN model's accuracy at different SOC levels. Finally, restrictions of the proposed model and future works are discussed.

## II. LITHIUM-SULFUR CELL

The lithium-sulfur cells investigated in this study are developed by OXIS Energy Ltd. Fig. 1 illustrates a 3.4 A·h Li-S cell and schematic of inside the cell, with the specifications listed in Table I. These Li-S cells have advantages over existing Li-ion cells, as follows [12]:

- 1) *High energy density*: high energy density: the cell manufacturer projects that the realizable specific energy for a Li-S cell will increase to 650 W·h/kg within a few years; this compares well to a figure of 250 W·h/kg for a Li-ion cell. The prototype Li-S cell which is tested in this study has energy density of 137 W·h/kg which is still far from the final target.

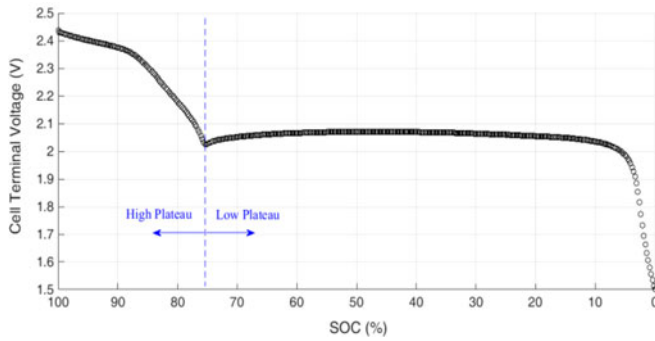


Fig. 2. Li-S cell terminal voltage during continuous discharge test at C/30 discharge rate.

- 2) *Improved safety*: protective layer over the lithium, high flash point electrolyte and no dendrite growth are the reasons that improve Li-S cell's safety in comparison to Li-ion cells.
- 3) *Lower environmental impact*: Sulfur, as the cathode material, is non-toxic and environmentally benign.
- 4) *Cost competitive*: in comparison to Li-ion cells, the different cathode material in Li-S cells, that is sulfur, is abundant and cheap.

Although the construction of a Li-S cell is similar to a Li-ion cell, the chemical reactions that take place inside the two cells and consequently their performances are very different. As illustrated in Fig. 1, a Li-S cell consists of different layers including: 1) A lithium metal anode, 2) A sulfur-based cathode, which includes carbon or a polymer binder, and 3) A non-flammable electrolyte rendering the cell inherently safe. Various reactions may take place inside a Li-S cell; the discharge process includes gradual reduction of sulfur to various polysulfides and finally to the low-order polysulfides and lithium sulfide, and oxidation of lithium metal to lithium ions. The opposite direction, that is charging, consists of reduction of the lithium ions to lithium, and oxidation of the sulfide and low order polysulfides to the higher-order polysulfides and sulfur [5]. These various reactions, at different charge levels, cause that Li-S cell's behaviour highly depends on SOC. A slow-discharge curve of the Li-S cell at C/30 discharge rate is illustrated in Fig. 2 where the cell's voltage changes from 2.45 V at fully charged state to 1.5 V at depleted state. Li-S cell's discharge curve can be divided into two separate parts which are high plateau (HP) and low plateau (LP) as shown in the figure. More details about the electrochemical reactions taking place inside a Li-S cell can be found in [13]–[15].

### III. METHODOLOGY

For Li-S cell model parameterization, this study has used formal 'system identification' techniques from control theory. A schematic showing the system identification process as a 'loop' is illustrated in Fig. 3 based on a concept developed by Ljung in [16]. In this concept, three main parts of a system identification process are as follows:

- 1) Model structure selection,

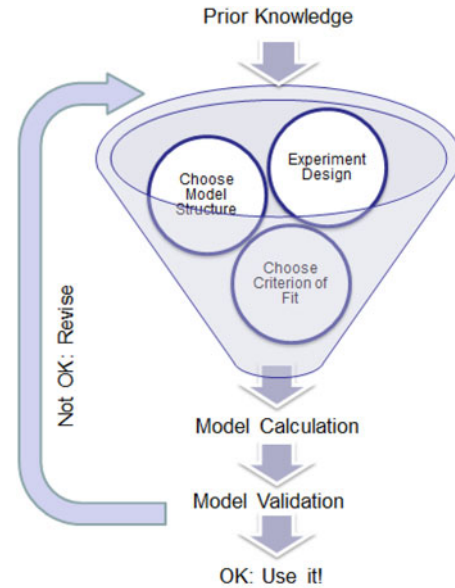


Fig. 3. System identification loop.

- 2) Experiment design, and
- 3) Fitness criterion and algorithm selection.

The methodology of this study follows this order. First, the ECN model structures to be considered for Li-S cell modelling are introduced. Then, experimental tests, which are designed for cell model identification, are presented and test equipment is described. Finally, the fitness criterion and identification algorithm to be used for cell model parameterization, are explained.

#### A. ECN Model Structures

ECN modelling is a common battery modelling technique in the literature. Having less complexity than electrochemical models, ECN models have been used in a wide range of applications and for various battery types [18], [19]. ECN models are constructed by putting resistors, capacitors and voltage sources in a circuit. The simplest form of an ECN battery model is 'R<sub>int</sub> model' or simply saying 'R model' [20]. The R model includes an ideal voltage source ( $V_{OC}$ ) and a resistor as depicted in Fig. 4(a): here R is the total battery resistance,  $V_t$  is the battery terminal voltage and  $I_L$  is the load current. Adding one RC network to the R model potentially increases its accuracy by allowing the model to reflect the polarization characteristics of the cell. A first order RC model or 'Thevenin' model [21], which has one RC network and a resistor as shown in Fig. 4(b), has been used in a wide range of applications in the literature [5]. In a RC model,  $V_t$  is terminal voltage,  $V_{OC}$  is open circuit voltage (OCV),  $R_O$  is ohmic resistance,  $R_P$  and  $C_P$  are equivalent polarization resistance and capacitance respectively. Adding more RC networks to the battery model may improve the accuracy; however, an appropriate compromise is needed between accuracy and simplicity of the model especially for real-time applications. In this study, four model structures are assessed as illustrated in Fig. 4(a)–(d) which are called here as R, 1RC, 2RC and 3RC models. Differential equations of an

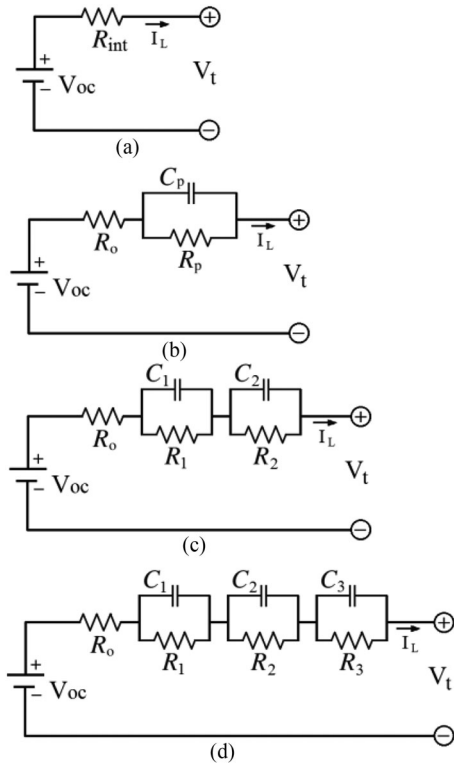


Fig. 4. Cell ECN models: (a) R model, (b) 1RC, (c) 2RC, and (d) 3RC.

ECN model with  $N$  networks like shown in Fig. 4 are:

$$\begin{cases} V_t = V_{OC} - R_O I_L - \sum_{i=1}^N V_{P_i} \\ \frac{dV_{P_i}}{dt} = -\frac{1}{R_{P_i} C_{P_i}} V_{P_i} + \frac{1}{C_{P_i}} I_L \quad (for \ i = 1..N) \end{cases} \quad (1)$$

### B. Experimental Tests

The second part of the model identification process, experimental test, was designed so that covers various battery operating conditions. All the tests were carried out on 3.4 Ah long life Li-S cells with specifications mentioned in Table 1, produced by OXIS Energy Ltd.

Series-4000 battery tester was used for the experiments. The battery tester is a voltage/current device that applies a current profile and measures the voltage or vice versa. Li-S cells were contained inside an aluminium test box connected to the equipment using crocodile clips. The boxes were inside a Binder thermal chamber to set the desired temperature during each test as depicted in Fig. 5.

Fig. 6 shows a mixed charge-discharge pulse test which was used for Li-S cell model parameterization in this study. Pulse tests are common in the literature to be used for modelling of various battery types. The pulse tests used in this study were based on those used by the cell manufacturer, and were intended to give data sets that allow the dynamics of interest to be clearly seen. (There is nothing particularly special about these choices, and it may well be possible to use a common standard pulse sequence for a Li-S cell as well.)

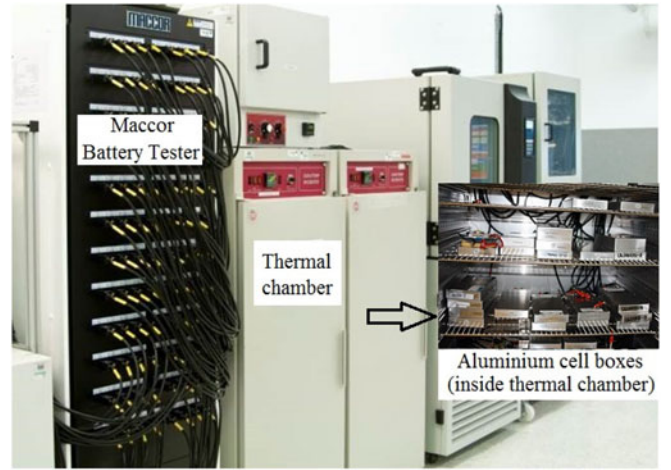


Fig. 5. Cell test equipment.

In this test, various charge/discharge rates and different SOC levels are taken into consideration. The test started at full charge state (2.45 V) and continued until the cell's terminal voltage dropped below 1.5 V (i.e. the cut-off voltage) which means a depleted state. Consecutive charge/discharge current pulses were applied to the cell as shown in the zoomed window in Fig. 6. The pulse sequence consists of 18 pulses (9 discharge and 9 charge pulses) including different frequencies and amplitudes. As shown in the figure, the whole pulse sequence was applied ten times at ten charge levels to investigate the effects of SOC. The models derived in this study represent a mix of discharge and charging behaviour: discharge is dominant, but there is a small amount of charging. This is chosen to simulate an EV driving scenario in which regenerative braking is modelled with charge pulses. Hysteresis effects are not explicitly modelled, and could be explored in future work.

The maximum current is not more than 1C because the Li-S cells used in this study were prototypes and they could not be subjected to higher currents. As the cell technologies mature, it is expected that higher currents will become practicable, and it will be possible to explore the sensitivities of model parameters to current and indeed other parameters.

Data was collected in the time domain with a sampling rate of 1 second. The measurements included time, current and the cell's terminal voltage while temperature was monitored to ensure that it is being kept constant by the test equipment. The test was repeated at various temperature levels including 10, 20, 30, 40 and 50 °C. Model parameterization was performed in each case, as described in the following sections.

### C. Fitness Criteria and Identification Algorithms

The well-known Prediction-Error Minimization (PEM) algorithm [16] is used for battery model parameterization. The algorithm minimizes the error (prediction error) between the ECN model's prediction and measurement. Operating over a short time interval; the PEM algorithm works on a small batch of data to find an estimate of the model's parameters. This is

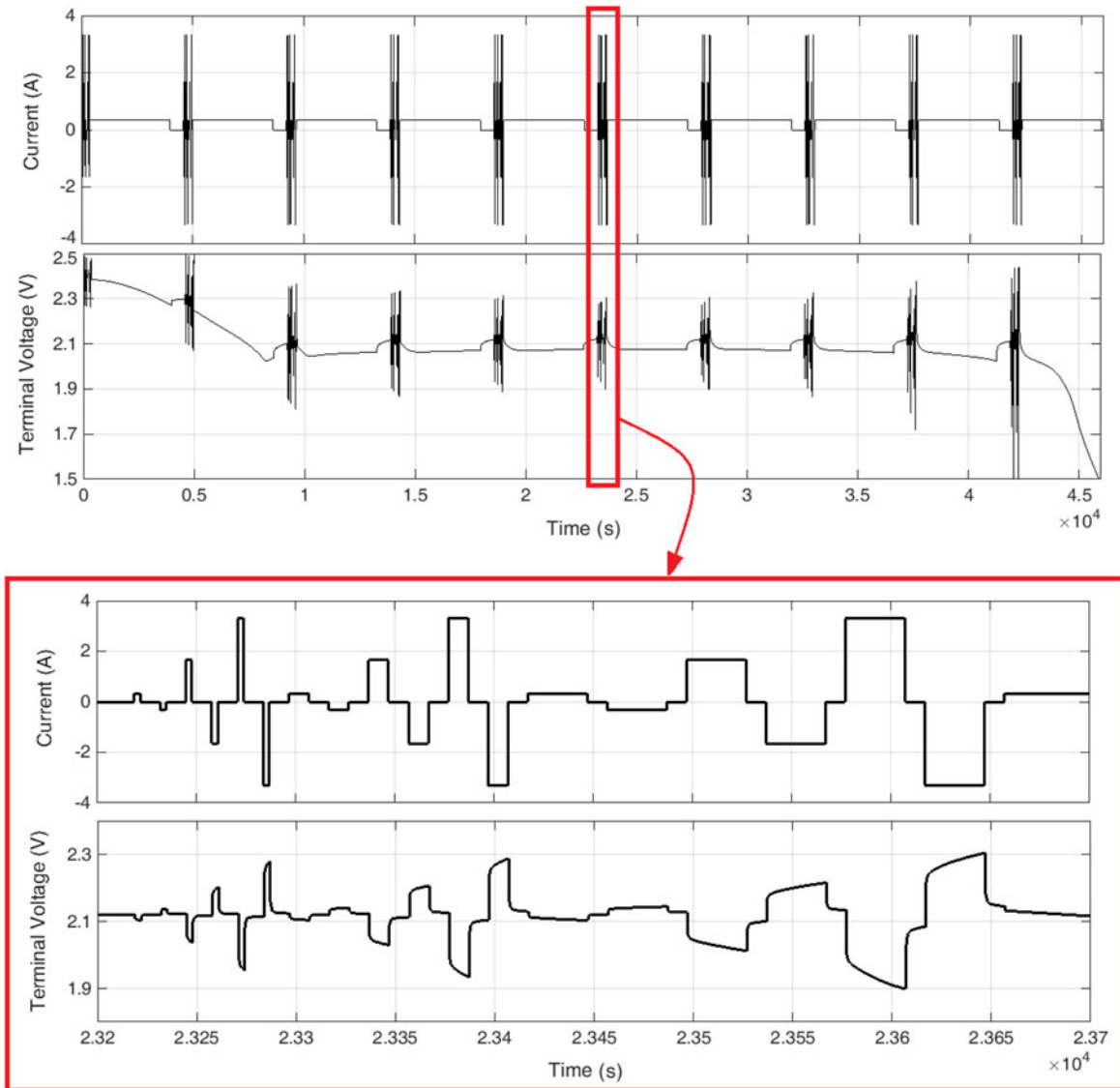


Fig. 6. Mixed charge/discharge impulse test.

carried out online but periodically and batch-wise rather than recursively: this approach is different from the on-line recursive algorithms that work based on sample point to sample point. For this specific application where the battery parameters are changing slowly with regard to SOC, temperature, etc., the PEM algorithm is fast enough to identify this time-varying model as discussed in [17]. So, the choice of PEM is reasonable because the measured data are assumed stationary and the battery model is assumed to be time-invariant within a short time interval. On the other hand, the algorithm does not have the limitations of the on-line algorithms which need time to settle, and do not always preserve all the dynamic information available.

It is assumed that the system ‘output’  $y(t_k)$  is a realization of a Gaussian stochastic process and it is stationary. The goal is to find a discrete-time model using the measurements of the process. The first step in our application is to determine the model’s structure which is one of the ECN models illustrated in

Fig. 4. During the identification procedure, the model’s parameter vector ( $\theta$ ) is determined so that the least difference between the process and model is achieved. So, here we are talking about a parameterization problem. In such a problem, prediction error ( $\varepsilon$ ) is defined as follows:

$$\varepsilon(t_k, \theta) = y(t_k) - \hat{y}(t_k | t_{k-1}; \theta) \quad (2)$$

where  $y(t_k)$  is the cell’s real output at time  $k$  and  $\hat{y}(t_k | t_{k-1}; \theta)$  is predicted value of the output at time  $k$  using the parameters vector  $\theta$ . The prediction error depends on the parameter vector, so an iterative minimization procedure has to be applied. Consequently a scalar fitness function is minimized as follows [16]:

$$E_N(\theta) = \det \left( \frac{1}{N} \sum_{k=1}^N \varepsilon(t_k, \theta) \varepsilon^T(t_k, \theta) \right) \quad (3)$$

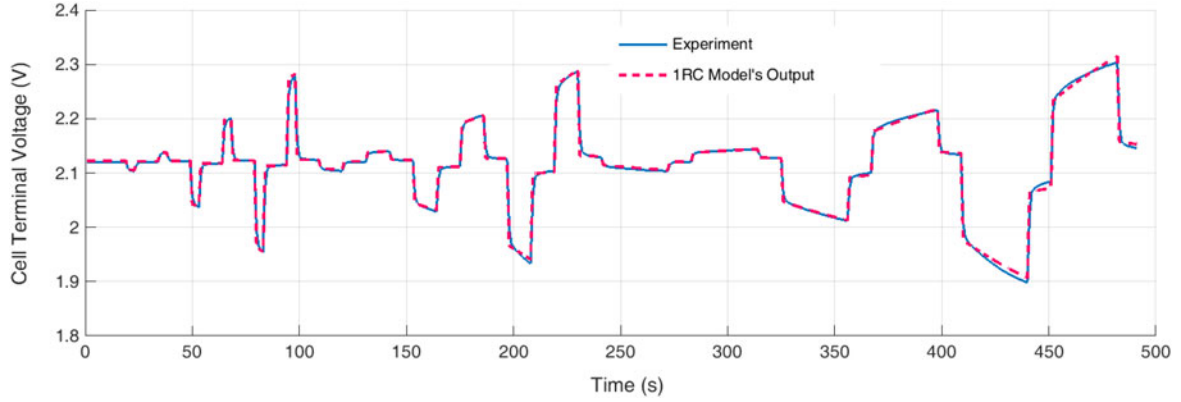


Fig. 7. Li-S cell's terminal voltage prediction using 1RC model.

The parameters are optimized so that the least difference between measured terminal voltage and the model's output is achieved. To evaluate the identification error,  $L_2$  and  $L^\infty$  norms were used as follows:

$$L_2 = \left[ \frac{1}{N} \sum_{k=1}^N |\varepsilon(t_k, \theta)|^2 \right]^{\frac{1}{2}} \quad (4)$$

$$L^\infty = \max_{k \in [1, N]} |\varepsilon(t_k, \theta)| \quad (5)$$

where  $L_2$  stands for root mean square error (RMSE) and  $L^\infty$  demonstrates maximum error value.

#### IV. RESULTS ANALYSIS

Referring to the mixed charge/discharge pulse test shown in Fig. 6, Li-S cell model identification was performed for all 10 pulse sequences shown in the figure. This means that the ECN model was parameterized every 10% change in SOC. The whole process was repeated for various model structures at different temperature levels. Consequently, different factors are considered including the effects of cell's model structure, SOC and temperature. Since the battery model's parameters are functions of SOC, which is not directly measurable, the model's sensitivity to the SOC estimation error is assessed as well. In the last section, restrictions of the proposed model are addressed.

##### A. Analysis of ECN Battery Model Structures

In Section III-A, four ECN models were introduced: simple resistance model (R model), 1RC model (Thevenin model), 2RC model and 3RC model. (The models are shown in Fig. 4). As discussed above, adding even more components to the model is possible however; it will be shown that increasing the complexity of the model is not necessarily beneficial. A goal of this study is to try different model structures for a Li-S cell during the model identification process. Accordingly, the average and maximum identification errors for the whole charge/discharge test were calculated for each model: these identification errors were the first criterion that was used to compare the models. Fig. 8 demonstrates how the identification accuracy depends on model structure. It was observed that the accuracy improved when more RC networks were added to the model. However,

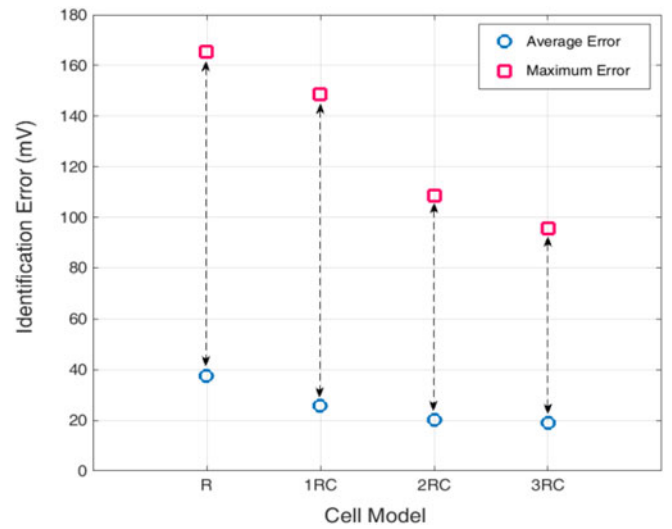


Fig. 8. Cell's terminal voltage prediction error using different models.

it should be noted that complexity and consequent computational effort was also increased. The computational time needed to perform identification—the 'identification time'—was taken as a second criterion for the models' evaluation. So a compromise must be made between accuracy and complexity for model structure selection.

Fig. 8 also demonstrates that the improvement caused by adding the first RC network to the model, is not the same as the second and third RC networks. In other words, there is not a big difference between the 2RC and 3RC models (average error of 20 mV for 2RC vs. 19 mV for 3RC) with regard to the identification accuracy. This result tells us that there is an optimal point that after it, more complexity will not necessarily result in more accuracy. In order to quantify the complexity of the models, the normalized value of the identification time was used: all the model structures were used for the same data set, the identification time was noted, and these time values were normalized by dividing by the maximum identification time. In this study, a pulse sequence was used. A sample 'batch' of the Li-S cell terminal voltage prediction using 1RC model is depicted in Fig. 7. (This is a part of the whole test shown in Fig. 6.) The process was repeated for all pulse sequences applied to

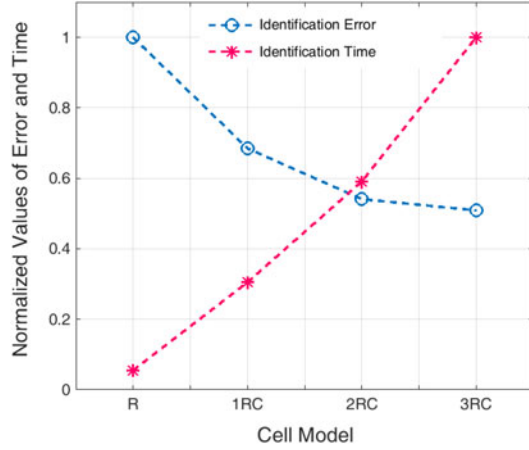


Fig. 9. Normalized cell's terminal voltage prediction error and identification time using different models.

the model structures. Average normalized identification time across the whole data sequence was obtained as presented in Fig. 9. The figure contains terminal voltage prediction error as well (normalized by its maximum value), so a trade-off can be explored between model's accuracy and speed. Based on the results presented in Fig. 9, if normalized time and normalized error are considered to be equally important, it is concluded that 2RC model would be a good compromise in this case. Other models might be selected in other cases depending on the modelling purpose. Application-oriented trade-offs between accuracy and speed in battery modelling has been discussed more deeply in [17].

### B. Analysis of the Effect of SOC

Before analysing the role of SOC in a Li-S cell model, a definition of battery SOC is presented. A common technique of battery SOC calculation, which is used as a benchmark in this area, is coulomb-counting. In this method, battery SOC is calculated by integrating the load current to know how much capacity is used and remained. Assuming  $SOC_0$  as the initial SOC at time  $t_0$ , battery SOC at time  $t$  is calculated as follows:

$$SOC = SOC_0 - \left( \int_{t_0}^t \frac{\gamma i(\tau)}{C_t} d\tau \right), \quad 0 < SOC < 1 \quad (6)$$

where  $i(t)$  is the current (A) assumed positive for discharging and negative for charging.  $\gamma$  is battery's coulombic efficiency (dimensionless) and  $C_t$  is the total capacity (As). In this representation, SOC value is a number between 0 and 1, where 0 indicates a fully depleted state and 1 represents a fully charged state.

In this study, the tests started at fully charged state (2.45 V) and continued until the cell's terminal voltage dropped below 1.5 V (i.e. the cut-off voltage) which means a depleted charge state. In this way, the whole discharge capacity ( $C_t$ ) is obtained after each test and is used for SOC calculation.

It was expected that SOC would affect a battery's dynamic behaviour, and this is confirmed by our test results. Fig. 10 shows how an ECN model's components are related to the behaviour

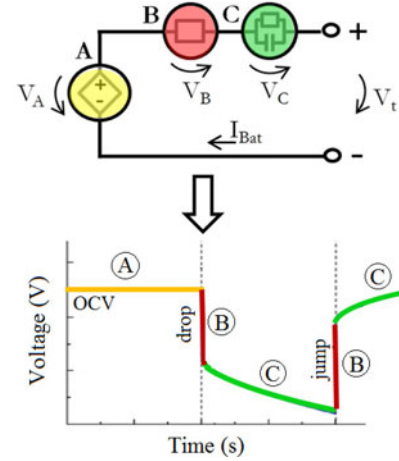


Fig. 10. Correlation between ECN model's components and different parts of the battery response subject to a discharge current pulse.

seen in a discharge current pulse. Each circuit parameter is dependent on SOC—as an example, the SOC-dependence of ohmic resistance ( $R_O$ ) and open circuit voltage ( $V_{OC}$ ), for a single temperature point is presented in Table II. When a current pulse is applied or removed, there is an instantaneous change in voltage equal in magnitude to the product of the ohmic resistance and the applied/removed current, as indicated in Fig. 10. So the ohmic resistance is calculated as follows:

$$R_O = \frac{|V_{t,k} - V_{t,k+1}|}{|I_{L,k} - I_{L,k+1}|} \quad (7)$$

where the load current is changed from  $I_{L,k}$  to  $I_{L,k+1}$  at time  $k$  and,  $V_{t,k}$  and  $V_{t,k+1}$  are cell's terminal voltage just before and after changing the current. On the other hand, open circuit voltage is the measured voltage when the battery is in relaxation, i.e. the load current is zero and steady-state has been reached.

The results demonstrate that Li-S cell's ohmic resistance has a highly nonlinear relationship with SOC as presented in Fig. 11 (the effect of temperature will be discussed later). Ohmic resistance is low at high SOC, increasing linearly in the high plateau (HP) by charge depleting. There is a break-point at the end of HP where cell's ohmic resistance starts decreasing after it. In the low plateau (LP), Li-S cell's ohmic resistance almost has a parabolic shape with a minimum point in the middle. The biggest value of ohmic resistance is at very low SOC.

### C. Analysis of the Effect of Temperature

In this section, the effect of temperature on Li-S cell's behavior is investigated. For this purpose, the mixed charge/discharge test was repeated at 10, 20, 30, 40 and 50 °C. Firstly, the relationship between cell's capacity and temperature was assessed. As demonstrated in Fig. 12, the Li-S cell's capacity decreases at low temperature (less than 30 °C) and it remains almost constant at high temperature. In order to double-check this result, the tests were repeated for another cell which confirms it as illustrated in Fig. 12.

The relationship between cell's ohmic resistance and temperature has been investigated too. Fig. 11 demonstrates Li-S cell's

TABLE II  
OPEN CIRCUIT VOLTAGE AND OHMIC RESISTANCE OF LI-S CELL AT DIFFERENT CHARGE LEVELS

SOC (%)	95	85	75	65	55	45	35	25	15	5
$V_{OC}$ (V)	2.371	2.233	2.083	2.094	2.098	2.100	2.099	2.096	2.087	1.995
$R_O$ ( $\Omega$ )	0.039	0.078	0.079	0.068	0.059	0.054	0.053	0.058	0.077	0.140

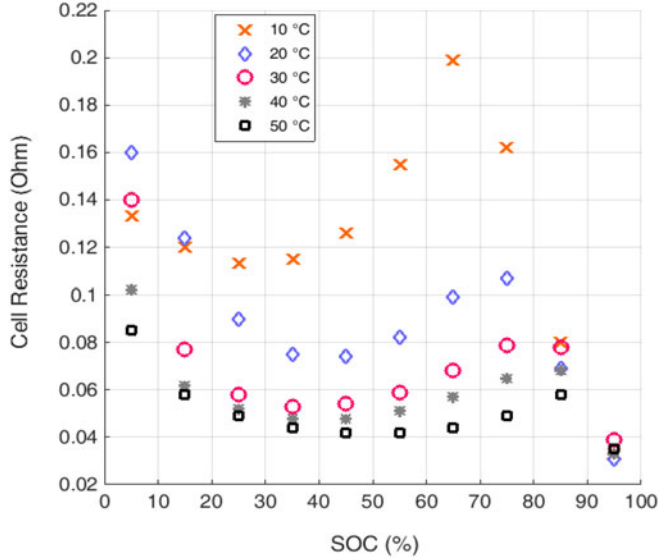


Fig. 11. Li-S cell's ohmic resistance vs. SOC at different temperatures.

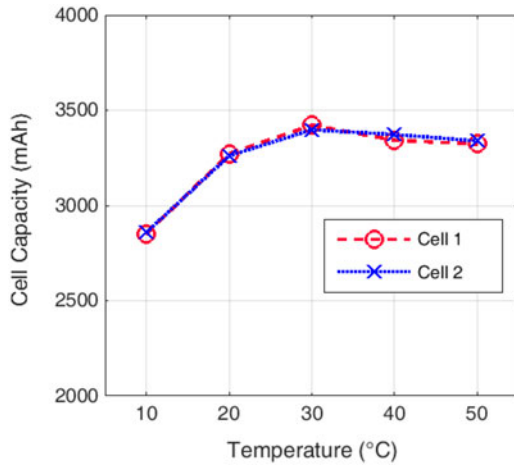


Fig. 12. Li-S cell's capacity at different temperature.

ohmic resistance vs. SOC at different temperature levels. This is a significant figure including a number of novel outcomes. Firstly, variation of cell's ohmic resistance vs. SOC follows a particular nonlinear pattern at all temperature levels (explained in Section IV-B). The second outcome is the effect of the temperature on cell's ohmic resistance. Generally, temperature and Li-S cell's ohmic resistance are inversely proportional. (Fig. 13 depicts variation of the maximum and average Li-S cell's ohmic resistance vs. temperature.) The third outcome of Fig. 11 is related to the effect of temperature on 'plateau change' in Li-S cell. As demonstrated in Fig. 2, there is a break-point between

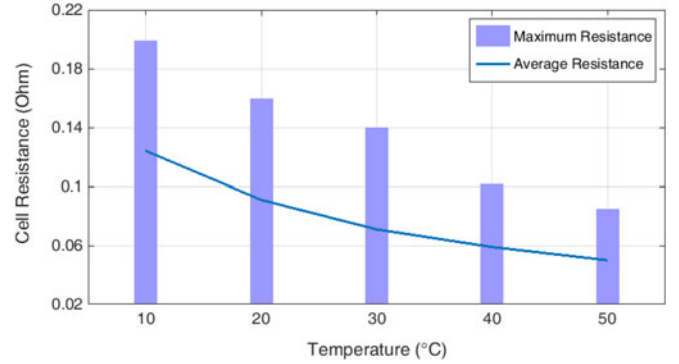


Fig. 13. Variation of the maximum and average Li-S cell's ohmic resistance vs. temperature.

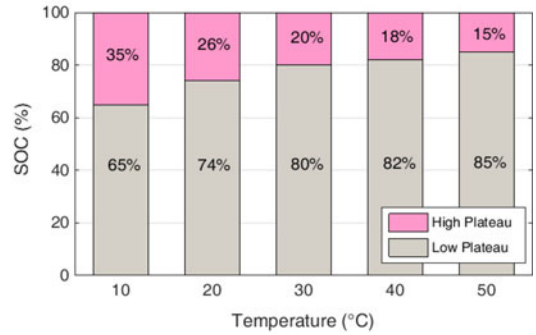


Fig. 14. Influence of temperature on plateau change in a Li-S cell.

HP and LP regions around 70% to 80% SOC due to a change in the reactions inside the cell as explained in Section II. The break-point is also detectable using ECN modelling approach where model's parameters have a harsh gradient change as depicted for ohmic resistance in Fig. 11. Because of the limited number of identification points in the figure, a curve fitting technique is needed to detect the exact location of the break-point. Fig. 14 demonstrates how temperature affects the location of the break-point where plateau changes. The results demonstrate that HP region shrinks as the temperature increases. The break-point moves from 65% at 10 °C to 85% at 50 °C.

#### D. Sensitivity Analysis of the Li-S Model to SOC Estimation Error

The proposed model can be mathematically presented in form of polynomial functions or lookup tables. In both cases, the cell model's parameters are functions of temperature and SOC. Temperature is usually available using an accurate sensor; however cell's SOC is not measurable directly and should be estimated. In



Section IV-B, coulomb-counting technique was used to calculate SOC. Although coulomb-counting is a quite useful technique, it suffers from practical limitations. For example, it can only start to estimate from a given initial SOC value. In many applications, batteries do not begin to discharge from fully charged state due to internal self-discharge or being not originally fully charged [22]. In addition, coulomb-counting technique suffers from accumulated errors caused by initial SOC value errors, and noise and measurement errors [23], [24]. Another problem is that the battery capacity ( $C_t$ ) might change under various conditions (e.g. temperature variation) which can lead to estimation errors when using coulomb-counting. A more reliable SOC estimation can be provided by using other techniques such as open-circuit voltage method, Kalman filter-based methods, etc. Good reviews of battery SOC estimation methods can be found in [25] and [26]. Even using more advanced battery SOC estimation algorithms, small errors are inevitable. Explanation of SOC estimation methods is out of the framework of this study however, sensitivity analysis of the proposed model to SOC estimation error is performed here. Indeed, it would be helpful to know how well the model performs if the correct value of SOC is not available. In order to investigate the sensitivity of the model to SOC, gradient of the model's error ( $L_2$ ) with respect to SOC was analysed. It is clear that the model's accuracy is affected by changing its parameters which are functions of SOC, temperature, etc. as follows:

$$P_i = f_i(SOC, T, \dots), \quad i = 1, 2, \dots, n \quad (8)$$

where  $P_i$  is a parameter of the model, T stands for temperature and n is the number of parameters used in the model. So, we can investigate the effect of SOC on the model's accuracy by using the formula in below. It says that the model's sensitivity to SOC is proportional to the sensitivity with respect to each parameter multiplied by the sensitivity of that parameter to SOC.

$$\frac{\partial L_2}{\partial SOC} \propto \sum_{i=1}^n \left( \frac{\partial L_2}{\partial P_i} \times \frac{\partial P_i}{\partial SOC} \right) \quad (9)$$

Assuming that  $R_O$  and  $V_{OC}$  are more influential in model's accuracy than  $R_1$  and  $C_1$ , equation (9) is simplified as follows:

$$\frac{\partial L_2}{\partial SOC} \propto \frac{\partial L_2}{\partial R_O} \times \frac{\partial R_O}{\partial SOC} + \frac{\partial L_2}{\partial V_{OC}} \times \frac{\partial V_{OC}}{\partial SOC} \quad (10)$$

At first, derivative of cell's ohmic resistance with respect to SOC ( $\partial R_O / \partial SOC$ ) is calculated at different charge and temperature levels as illustrated in Fig. 15 (absolute values are shown in the figure). The dashed line just shows the general trend which is the average of all temperature levels. The results demonstrate that Li-S cell's ohmic resistance changes fast at low and high SOC regions. So regarding the ohmic resistance only, the model is more sensitive to SOC estimation error at low and high charge levels. However, it should be noted that the open circuit voltage can also affect the overall results. Referring to Fig. 2, open circuit voltage changes much faster in HP than LP. It means that the derivative of cell's open circuit voltage with respect to SOC ( $\partial V_{OC} / \partial SOC$ ) has higher values at HP. For investigation of the resultant effect of the two factors ( $R_O$  and  $V_{OC}$ ) simultaneously, a specific analysis is conducted.

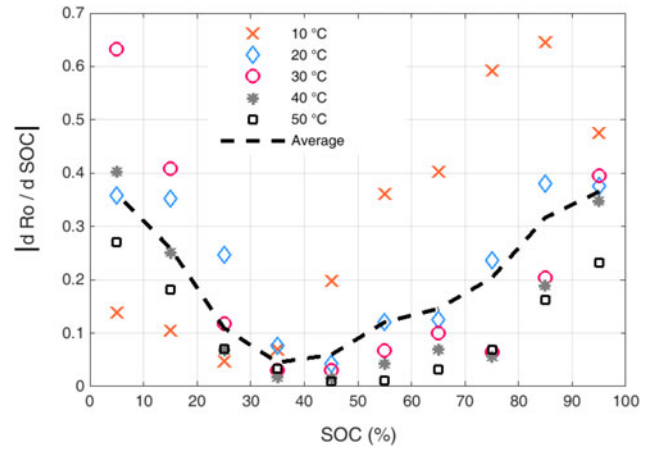


Fig. 15. Derivative of Li-S cell ohmic resistance over SOC at different charge and temperature levels.

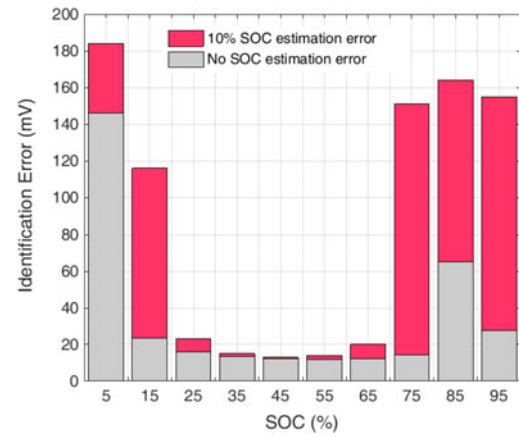


Fig. 16. Cell terminal voltage prediction error with and without SOC estimation error.

Referring back to Fig. 8 (cell's terminal voltage prediction error), it should be noted that the results were obtained using an 'ideal model'. Here 'ideal model' means a model whose parameters are optimised for that particular case without any error in SOC estimation. However in a real application, an error in SOC estimation is inevitable. For our analysis, the results are calculated again using an 'not-ideal model' with 10% deviation in SOC from its correct value.—Fig. 16 demonstrates the effect of SOC estimation error on model's accuracy. The cell's terminal voltage prediction error is obtained with 10% SOC error and it is plotted against the ideal model. In this analysis, the simplest form of the cell models [shown in Fig. 4(a)] was used. The results demonstrate that the Li-S cell model has the most sensitivity to SOC estimation error around the break-point (75% to 80% SOC at 30 °C). The next highest sensitivity is at low and high charge levels. It is concluded that SOC estimation accuracy is less vital in middle SOC range from 20% to 70%.

#### E. Limitations of the Proposed Model

There are a number of limitations for the proposed model in this study. The capacity fade in a Li-S cell is a challenging issue for automotive application. Li-S cell capacity fade occurs due

to cell ageing (cycling). So, an ageing factor should also be considered in the model in addition to SOC and temperature. For more detail, Li-S cell capacity fade due to cycling is addressed in [9], [10], and [27]. A Li-S cell's capacity might decrease because of the composition change on the surface of the lithium electrode and formation of a layer of solid products on the surface of the sulfur electrode during cycling. In detail, whereas the polysulfides  $S_8^{-2}$ ,  $S_6^{-2}$ , and  $S_4^{-2}$  are soluble in the electrolyte, the polysulfide ions  $Li_2S_2$  and  $Li_2S$  are relatively insoluble. So they might remain within the body of the positive electrode. The shuttling of polysulfides between the electrodes is a major technical issue limiting the self-discharge and cycle life of the Li-S battery [28]. Shuttle phenomenon has been investigated in previous studies [29]–[31] and research in this area is ongoing.

### V. CONCLUSIONS

In this study, ECN modelling of a Li-S cell was investigated. Model parameterization was performed under various conditions. The results were analysed by considering different aspects such as the effects of model structure, SOC and the ambient temperature. In addition, sensitivity of the proposed model's accuracy to SOC estimation error was assessed and limitations of the model were identified and discussed. All in all, the following outcomes can be highlighted as main conclusions of this study:

- 1) A proper compromise between accuracy and complexity in selection of an ECN model structure for Li-S cell has been explored. It was concluded that the 2RC model is a good general compromise, giving good accuracy and speed. However, other model structures might be more appropriate in other applications depending on the aims of modelling and the criteria for 'goodness'.
- 2) The model identification results demonstrated that a Li-S cell's ohmic resistance is low at high SOC, where it increases linearly in 'high plateau' region (by charge depletion). There is a break-point at the end of high plateau where cell's ohmic resistance starts decreasing. In the 'low plateau', the graph of a cell's ohmic resistance has a near parabolic shape with a minimum point near the centre of the low plateau; after that, the Li-S cell has the greatest ohmic resistance value at very low SOC. However, at low temperature, the maximum ohmic resistance occurs just at the break-point between high plateau and low plateau as demonstrated in Fig. 11 for 10 °C.
- 3) The effect of temperature on a Li-S cell's behaviour was investigated and the following patterns were observed: a Li-S cell's capacity decreases at low temperature, but above the ambient temperature it remains almost constant, with only a small drop as temperature increases. The temperature and ohmic resistance were found to be approximately inversely proportional. Changes in temperature were found to have an effect on the shape of the 'high plateau', which was observed to shrink as the temperature increased.
- 4) Finally, a sensitivity analysis showed that the Li-S cell model's accuracy was most sensitivity to SOC estimation error around the break-point; the next most sensitive SOC

regions were at high and low SOC range. It was concluded that in consequence, SOC estimation accuracy was less critical in middle SOC range, i.e. 20% to 70%.

### ACKNOWLEDGMENTS

Enquiries for access to the data referred to in this article should be directed to . The underlying data can be accessed through the Cranfield University data repository at <http://dx.doi.org/10.17862/cranfield.rd.c.3707182>.

### REFERENCES

- [1] C. Barchasz, F. Molton, C. Duboc, J. C. Lepretre, S. Patoux, and F. Alloin, "Lithium/sulfur cell discharge mechanism: An original approach for intermediate species identification," *Anal. Chem.*, vol. 84, pp. 3973–3980, 2012.
- [2] C. E. Thomas, "Fuel cell and battery electric vehicles compared," *Int. J. Hydrogen Energy*, vol. 34, pp. 6005–6020, 2009.
- [3] V. S. Kolosnitsyn, "Lithium-sulfur batteries: Problems and solutions," *Russ. J. Electrochem.*, vol. 44, pp. 506–509, 2008.
- [4] K. Kumaresan, Y. Mikhaylik, and R. E. White, "A mathematical model for a lithium-sulfur cell," *J. Electrochem. Soc.*, vol. 155, no. 8, pp. A576–A582, 2008.
- [5] A. Fotouhi, D. J. Auger, K. Propp, S. Longo, and M. Wild, "A review on electric vehicle battery modelling: From lithium-ion toward lithium-sulfur," *Renewable Sustain. Energy Rev.*, vol. 56, pp. 1008–1021, 2016.
- [6] J. Chiasson and B. Vairamohan, "Estimating the state of charge of a battery," *IEEE Trans. Control Syst. Technol.*, vol. 13, no. 3, pp. 465–470, May 2005.
- [7] C. Antaloae, J. Marco, and F. Assadian, "A novel method for the parameterization of a Li-ion cell model for EV/HEV control applications," *IEEE Trans. Veh. Technol.*, vol. 61, no. 9, pp. 3881–3892, Nov. 2012.
- [8] B. R. K. Schweighofer and G. Brasseur, "Modeling of high power automotive batteries by the use of an automated test system," *IEEE Trans. Instrum. Meas.*, vol. 52, no. 4, pp. 1087–1091, Aug. 2003.
- [9] V. S. Kolosnitsyn, E. V. Kuz'mina, E. V. Karaseva, and S. E. Mochalov, "Impedance spectroscopy studies of changes in the properties of lithium-sulfur cells in the course of cycling," *Russ. J. Electrochem.*, vol. 47, no. 7, pp. 793–798, 2011.
- [10] V. S. Kolosnitsyn, E. V. Kuz'mina, E. V. Karaseva, and S. E. Mochalov, "A study of the electrochemical processes in lithium-sulfur cells by impedance spectroscopy," *J. Power Sources*, vol. 196, pp. 1478–1482, 2011.
- [11] V. Knap, D. I. Stroe, R. Teodorescu, M. Swierczynski, and T. Stanciu, "Electrical circuit models for performance modeling of lithium-sulfur batteries," in *Proc. IEEE Energy Convers. Congr. Expo.*, Montreal, QC, Canada, 2015, pp. 1375–1381.
- [12] (2016). [Online]. Available: <http://www.oxisenergy.com>
- [13] Y. Lia, H. Zhan, S. Liu, K. Huang, and Y. Zhou, "Electrochemical properties of the soluble reduction products in rechargeable Li/S battery," *J. Power Sources*, vol. 195, pp. 2945–2949, 2010.
- [14] J. P. Neidhardt, D. N. Fronczek, T. Jahnke, T. Danner, B. Horstmann, and W. G. Bessler, "A flexible framework for modeling multiple solid, liquid and gaseous phases in batteries and fuel cells," *J. Electrochem. Soc.*, vol. 159, no. 9, pp. A1528–A1542, 2012.
- [15] M. Ghaznavi and P. Chen, "Sensitivity analysis of a mathematical model of lithium-sulfur cells part I: Applied discharge current and cathode conductivity," *J. Power Sources*, vol. 257, pp. 394–401, 2014.
- [16] L. Ljung, *System Identification—Theory for the User*. New York, NY, USA: Prentice-Hall, 1987.
- [17] A. Fotouhi, D. J. Auger, K. Propp, and S. Longo, "Accuracy versus simplicity in online battery model identification," *IEEE Trans. Syst., Man, Cybern., Syst.*, 2016, pp. 1–12, doi: 10.1109/TSMC.2016.2599281.
- [18] A. Fotouhi, K. Propp, and D. J. Auger, "Electric vehicle battery model identification and state of charge estimation in real world driving cycles," in *Proc. Comput. Sci. Electron. Eng. Conf.*, Colchester, U.K., 2015, pp. 243–248.
- [19] H. He, R. Xiong, X. Zhang, F. Sun, and J. X. Fan, "State-of-charge estimation of the lithium-ion battery using an adaptive extended kalman filter based on an improved Thevenin model," *IEEE Trans. Veh. Technol.*, vol. 60, no. 4, pp. 1461–1469, May 2011.

- [20] V. H. Johnson, "Battery performance models in ADVISOR," *J. Power Sources*, vol. 110, pp. 321–329, 2002.
- [21] Z. M. Salameh, M. A. Casacca, and W. A. Lynch, "A mathematical model for lead-acid batteries," *IEEE Trans. Energy Convers.*, vol. 7, no. 1, pp. 93–98, Mar. 1992.
- [22] C.H. Cai, D. Du, and Z. Y. Liu, "Battery state-of-charge (SOC) estimation using adaptive neuro-fuzzy inference system (ANFIS)," in *Proc. 12th IEEE Int. Conf. Fuzzy Syst.*, 2003, vol. 2, pp. 1068–1073.
- [23] B. Pattipati, C. Sankavaram, and K. Pattipati, "System identification and estimation framework for pivotal automotive battery management system characteristics," *IEEE Trans. Syst., Man, Cybern. C, Appl. Rev.*, vol. 41, no. 6, pp. 869–884, Nov. 2011.
- [24] K. Kutluay, Y. Cadirci, Y. S. Ozkazanc, and I. Cadirci, "A new online state-of-charge estimation and monitoring system for sealed lead-acid batteries in telecommunication power supplies," *IEEE Trans. Ind. Electron.*, vol. 52, no. 5, pp. 1315–1327, Oct. 2005.
- [25] S. Pillar, M. Perrin, and A. Jossen, "Methods for state-of-charge determination and their applications," *J. Power Sources*, vol. 96, pp. 113–120, 2001.
- [26] M. Ugras Cuma and T. Koroglu, "A comprehensive review on estimation strategies used in hybrid and battery electric vehicles," *Renewable Sustain. Energy Rev.*, vol. 42, pp. 517–531, 2015.
- [27] V. S. Kolosnitsyn, E. V. Karaseva, and A. L. Ivanov, "Electrochemistry of a lithium electrode in lithium polysulfide solutions," *Russ. J. Electrochem.*, vol. 44, no. 5, pp. 564–569, 2008.
- [28] D. Moy, A. Manivannan, and S. R. Narayanan, "Direct measurement of polysulfide shuttle current: A window into understanding the performance of lithium-sulfur cells," *J. Electrochem. Soc.*, vol. 162, no. 1, pp. A1–A7, 2015.
- [29] Y. Diao, K. Xie, S. Xiong, and X. Hong, "Shuttle phenomenon—The irreversible oxidation mechanism of sulfur active material in Li-S battery," *J. Power Sources*, vol. 235, pp. 181–186, 2013.
- [30] A. F. Hofmann, D. N. Fronczek, and W. G. Bessler, "Mechanistic modeling of polysulfide shuttle and capacity loss in lithium sulfur batteries," *J. Power Sources*, vol. 259, pp. 300–310, 2014.
- [31] M. R. Busche, P. Adelhelm, H. Sommer, H. Schneider, K. Leitner, and J. Janek, "Systematical electrochemical study on the parasitic shuttle-effect in lithium-sulfur-cells at different temperatures and different rates," *J. Power Sources*, vol. 259, pp. 289–299, 2014.

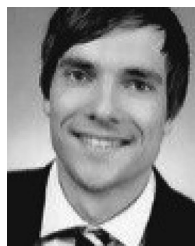


**Abbas Fotouhi** received the Ph.D. degree in mechanical engineering from Iran University of Science and Technology. He is a Research Scientist in the field of transportation engineering and vehicle technology. He started his academic career as a Lecturer at Islamic Azad University, Iran, in 2011. He then joined the Centre for Artificial Intelligence and Robotics, University Technology Malaysia. Since 2014, he has been with the Advanced Vehicle Engineering Centre, Cranfield University, where he is doing research, teaching and supervising postgraduate students.

His specialty is modelling and simulation, identification, control and optimization. Artificial intelligence and machine learning are also part of his background. His current research is mainly focused on battery technology, vehicle powertrain design and optimization, and intelligent mobility.



**Daniel J. Auger** studied at Cambridge, U.K., where he received the M.Eng. and Ph.D. degrees in control engineering, specializing in model validation for robust feedback control design. He is currently a Lecturer of advanced control and optimization at Cranfield University, U.K. His current research interests include the application of advanced control methodologies to automotive design, development of software-embeddable battery models, optimal state-estimator design, and robust control architectures. His recent publications have looked at multiobjective optimization of electrified powertrains, embeddable models of lithium-sulfur batteries, and advanced techniques for battery state estimation.



**Karsten Propp** received the Master of Automotive Engineering degree from the University of Applied Sciences, Berlin, Germany, and is currently working toward the Ph.D. degree under the supervision of D. Auger in the Advanced Vehicle Engineering Centre, Cranfield University, U.K. His research focusses on the development of advanced control algorithms for vehicle battery management systems applicable for lithium sulfur cells.



**Stefano Longo** (SM'16) received the M.Sc. degree in control systems from the University of Sheffield, U.K., in 2007 and the Ph.D. degree in networked control systems from the University of Bristol, U.K., in 2011. He has been a Lecturer (Assistant Professor) of vehicle electronics and control at Cranfield University, U.K., since 2012. In November 2010, he was appointed to the position of a Research Associate at Imperial College London. He is currently the Course Director for the MSc in Automotive Mechatronics, an Associate Editor of the *Elsevier Journal*

*on Mechatronics*, an elected executive member of the Institution of Engineering and Technology (IET) Control and Automation Network, and a member of the IFAC technical committee on Mechatronic Systems. His Ph.D. thesis received the IET Control and Automation Prize for significant achievements in the area of control engineering.



**Rajlakshmi Purkayastha** received the B.Tech. degree in metallurgical engineering and materials science from the Indian Institute of Technology, Bombay, and the Ph.D. degree in materials science from the University of California, Santa Barbara, CA, USA, in 2013, specializing in micromechanical modelling of lithium ion battery storage particles. Following a postdoctoral position at Cambridge University running conducting research on the high velocity response of layered materials, she joined OXIS Energy in 2015. She is currently the Technical Lead for the

Revolutionary Electric Vehicle Battery Project, which is a multipartner collaboration funded by Innovate UK, which aims to develop lithium sulfur technology for automotive applications. Her current interests include thermal and degradation analysis of lithium sulfur batteries.



**Laura O'Neill** received the M.Chem. degree from the University of Liverpool, U.K., in 2010 and the D.Phil. degree from Oxford University, U.K., in 2014. Her D.Phil. degree was based on the materials science school and focused on nanostructured materials for energy storage applications. She then joined OXIS Energy as an Experimentalist, focusing on parameterizing and validating mechanistic models. She is currently the Technical Lead on a collaborative project developing lithium sulfur batteries for use in high-altitude pseudo satellites.



**Sylwia Waluś** received the European M.Sc. degree in 2010 under the MESC program, i.e., Materials for Energy Storage and Conversion. In 2011, she was a Research Scientist with CEA-Grenoble, France, exploring application of impedance technique for Li-ion batteries. Since 2011, her research has been oriented toward lithium-sulfur batteries, starting with the Ph.D. thesis (2011–2015) with the University of Grenoble and CEA-Grenoble, France, where she focused on a very fundamental aspect of this technology. From 2015, she has been with OXIS Energy as

a Research Scientist, where she is involved in more applied research and on the engineering side of Li-S cells. Her current work under the REVb project focuses on developing tests protocols adaptable for Li-S cells and characterization of precommercial prototypes, which provides support for modelling and BMS design for Li-S technology.